

**Evidence for different gravitational-wave sources in the NANOGrav dataset**Ligong Bian<sup>1,\*</sup>, Rong-Gen Cai<sup>2,3,4,†</sup>, Jing Liu<sup>4,3,‡</sup>, Xing-Yu Yang<sup>2,3,§</sup> and Ruiyu Zhou<sup>1,||</sup><sup>1</sup>*Department of Physics, Chongqing University, Chongqing 401331, China*<sup>2</sup>*CAS Key Laboratory of Theoretical Physics, Institute of Theoretical Physics, Chinese Academy of Sciences, P.O. Box 2735, Beijing 100190, China*<sup>3</sup>*School of Physical Sciences, University of Chinese Academy of Sciences, No.19A Yuquan Road, Beijing 100049, China*<sup>4</sup>*School of Fundamental Physics and Mathematical Sciences, Hangzhou Institute for Advanced Study, University of Chinese Academy of Sciences, Hangzhou 310024, China*

(Received 12 October 2020; accepted 12 March 2021; published 12 April 2021)

The NANOGrav Collaboration recently reported a strong evidence for a stochastic common-spectrum process in the pulsar-timing data. We evaluate the evidence of interpreting this process as mergers of super massive black hole binaries and/or various stochastic gravitational-wave background sources in the early Universe, including first-order phase transitions, cosmic strings, domain walls, and large amplitude curvature perturbations. We discuss the implications of the constraints on these possible sources. It is found that the data shows a positive evidence in favor of the cosmic strings against other gravitational-wave sources based on the Bayes factor analysis.

DOI: [10.1103/PhysRevD.103.L081301](https://doi.org/10.1103/PhysRevD.103.L081301)**I. INTRODUCTION**

Recently, with the 12.5-yr data set, the NANOGrav Collaboration reports a strong evidence of a stochastic common-spectrum process [1]. The process may be interpreted as gravitational waves (GWs) from mergers of supermassive black hole binaries (SMBHBs) [2–5] with a spectral index of 13/3 [1], or other speculative stochastic gravitational-wave backgrounds (SGWBs) in the nanohertz frequency region, such as cosmic strings [6], first-order phase transitions (FOPTs) [7,8], a primordial GW background produced by quantum fluctuations of the gravitational field during inflation [9], and domain walls [10].

Motivated by the observation, there are several attempts to interpret the results of GWs from supermassive black holes [11–13], cosmic strings [14–16], dark phase transition [17–19], and large scalar fluctuations associated with primordial black hole (PBH) formation [11,12]. In this letter, based on the assumption that the stochastic common-spectrum process is attributed to GWs, we first apply a Bayesian analysis to evaluate the strength of evidence for explaining the stochastic common-spectrum process with different models, including: SMBHBs, cosmic strings, scalar perturbations, FOPTs, domain walls, and/or a superposition of some of these GW sources above. We find out

the constraints on parameter spaces of these GWs models. The constraints on the gravitational-wave parameters from all these sources can be used to limit: 1) the phase transition parameters of the dark sector, 2) the symmetry breaking scale of new physics beyond the Standard Model of particle physics, and 3) the PBH abundance. Model comparisons of the Bayesian fit are performed to judge GW model interpretations with the current NANOGrav 12.5-yr data. Note that, here, the Bayesian analysis is conducted using the violin plots at the first five frequency bins in the left panel of Fig. 1 in Ref. [1] as data, instead of pulsar-timing data directly, and the assumption that using the spectral coefficients as independent data is taken.

**II. NANOGrAV 12.5-YR RESULTS VERSUS GW SOURCES**

We perform a Bayesian inference over the first five frequency bins of the NANOGrav 12.5-yr data set [1], roughly  $f \in (2.5 \times 10^{-9}, 1.2 \times 10^{-8})$  Hz. We apply the full Bayesian model fitting and model comparison procedure to these explanations. The free parameters of each model are set with uniform priors.

**A. GWs from FOPTs**

Two crucial parameters for the calculation of GWs from FOPTs are: 1) the latent heat [20],  $\alpha_{PT}$ , 2) the inverse time duration of the phase transition  $\frac{\beta}{H_n}$ , where  $T_n$  is the PT temperature and  $H_n$  is the Hubble parameter. We consider the nonrunaway bubbles where the GW sources from

\*lgbycl@cqu.edu.cn

†cairg@itp.ac.cn

‡liujing@ucas.ac.cn

§yangxingyu@itp.ac.cn

||zhouy@cqu.edu.cn

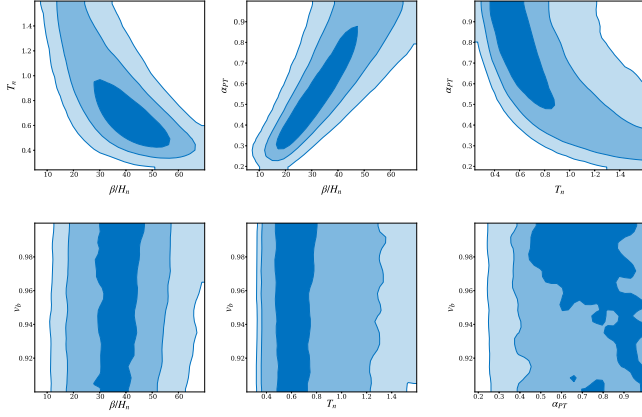


FIG. 1. Constraints on parameters of FOPTs from Bayesian model fitting. The contour levels in the plots correspond to the 1-, 2-, and 3- $\sigma$  levels in two-dimensional distributions.

FOPTs are dominated by sound waves, and the GW energy spectrum reads [20]

$$\Omega_{\text{GW}}^{\text{sw}} h^2(f) = 2.65 \times 10^{-6} (H_* \tau_{\text{sw}}) \left(\frac{\beta}{H_*}\right)^{-1} v_b \left(\frac{\kappa_\nu \alpha_{PT}}{1 + \alpha_{PT}}\right)^2 \times \left(\frac{g_*}{100}\right)^{-\frac{1}{3}} \left(\frac{f}{f_{\text{sw}}}\right)^3 \left(\frac{7}{4 + 3(f/f_{\text{sw}})^2}\right)^{7/2}. \quad (1)$$

Here, the factor  $\tau_{\text{sw}} = \min[\frac{1}{H_*}, \frac{R_*}{v_b}]$  is adopted to account for the duration of the phase transition [21–25], where  $H_* R_* = v_b (8\pi)^{1/3} (\beta/H_*)^{-1}$  [23] and the root-mean-square (rms) fluid velocity is  $\bar{U}_f^2 \approx \frac{3}{4} \frac{\kappa_\nu \alpha}{1 + \alpha}$  [24–26]. The factor  $\kappa_\nu$  is the fraction of the latent heat transferred into the kinetic energy of plasma, which is obtained by the hydrodynamic analysis [27]. The peak frequency of sound waves locates at  $f^{\text{sw}} = 1.9 \times 10^{-5} \frac{\beta}{H} \frac{1}{v_b} \frac{T_*}{100} \left(\frac{g_*}{100}\right)^{\frac{1}{6}}$  Hz [26,28,29]. For this study, we consider the plasma temperature being  $T_* \approx T_n$ .

In Fig. 1, we perform a whole parameter space scan, and the data constraints at  $1\sigma$  favors the following: a supersonic velocity  $v_b \sim [0.91, 0.99]$  and a moderate latent heat  $\alpha_{PT} \sim [0.31, 0.96]$ , with a duration  $\beta/H_n \sim [18.17, 58.27]$  at phase transition temperature  $T_n \sim [0.42, 1.43]$  MeV for the FOPT. We note that the big-bang nucleosynthesis (BBN) bounds  $T_* \geq 1$  MeV [30]. This result may invalidate a lot of parameter spaces of the dark phase transition explanation of the NANOGrav observation [17–19] at this level.

## B. GWs from cosmic strings

The vastly adopted Nambu-Goto cosmic strings are characterized solely by the dimensionless parameter  $G\mu$ , where  $G$  is Newton’s constant and  $\mu$  is the string tension, which is a function of the breaking scale of the  $U(1)$  symmetry. We consider GWs emitted by the cosmic string network are dominated by cusps here, with [31]  $\Omega_{\text{GW}}^{\text{cs}}(f) = \sum_k \Omega_{\text{GW}}^{(k)}(f)$ , and for each  $k$ -mode [32],

$$\Omega_{\text{GW}}^{(k)}(f) = \frac{1}{\rho_c} \frac{2k}{f} \frac{\mathcal{F}_\alpha \Gamma^{(k)} G \mu^2}{\alpha_{CS} (\alpha_{CS} + \Gamma G \mu)} \int_{t_F}^{t_0} d\tilde{t} \frac{C_{\text{eff}}(t_i^{(k)})}{t_i^{(k)4}} \times \left[\frac{a(\tilde{t})}{a(t_0)}\right]^5 \left[\frac{a(t_i^{(k)})}{a(\tilde{t})}\right]^3 \Theta(t_i^{(k)} - t_F). \quad (2)$$

Here,  $\rho_c = 3H_0^2/8\pi G$  is the critical density, and we take  $\mathcal{F}_\alpha = 0.1$  to characterize the fraction of the energy released by long strings. The loop production efficiency is adopted as  $C_{\text{eff}} = 5.4(0.39)$  in the radiation (matter) dominated universe [33]. The gravitational loop-emission efficiency is  $\Gamma \approx 50$  [35]. The fourier modes of cusps [36] are [35,37]  $\Gamma^{(k)} = \frac{\Gamma k^{\frac{4}{3}}}{\sum_{m=1}^{\infty} m^{\frac{4}{3}}}$ ; here,  $\sum_{m=1}^{\infty} m^{-\frac{4}{3}} \simeq 3.60$  and  $\sum_k \Gamma^{(k)} = \Gamma$ .

The formation time of loops of the  $k$ -mode casts the form of

$$t_i^{(k)}(\tilde{t}, f) = \frac{1}{\alpha_{CS} + \Gamma G \mu} \left[ \frac{2k}{f} \frac{a(\tilde{t})}{a(t_0)} + \Gamma G \mu \tilde{t} \right], \quad (3)$$

where  $\tilde{t}$  is the GW emission time. The cosmic string network reaches an attractor scaling solution after the formation time  $t_F$ . When the small-scale structure of loops is dominated by cusps, the high mode relates to the low mode as follows:  $\Omega_{\text{GW}}^{(k)}(f) = \frac{\Gamma^{(k)}}{\Gamma^{(1)}} \Omega_{\text{GW}}^{(1)}(f/k) = k^{-4/3} \Omega_{\text{GW}}^{(1)}(f/k)$ .

In Fig. 2 we show the results of Bayesian model fitting for the cosmic string network case. The constraints yield  $\log_{10} G\mu \sim [-10.44, -7.64]$  at  $1\sigma$ , which suggests the  $U(1)$  symmetry breaking scale of the new physics connecting with grand unification is around  $\eta \sim \mathcal{O}(10^{14-15})$  GeV for local strings (where  $\mu \approx 2\pi\eta^2$  for the winding number  $n = 1$ ), and  $\log_{10} \alpha_{CS} \sim [-3.91, -2.63]$  is allowed by data

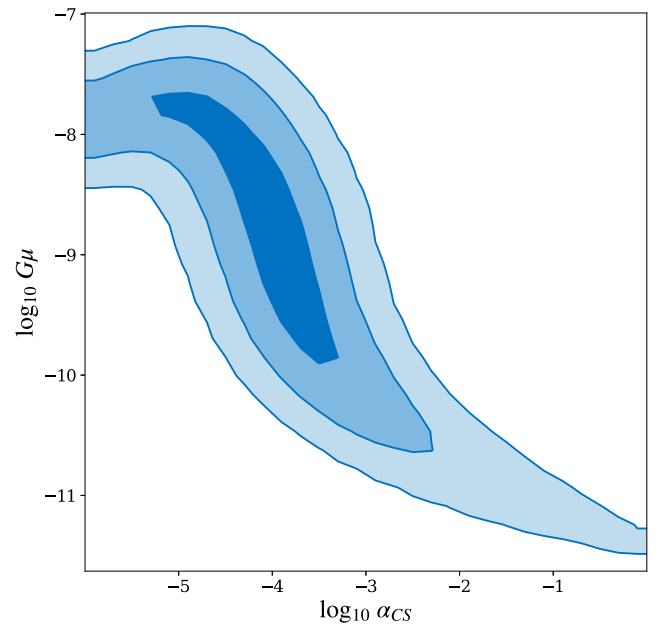


FIG. 2. Constraints on parameters of cosmic strings from the Bayesian model fitting.

at  $1\sigma$ , which is slightly smaller than the  $\alpha_{CS} = 0.1$  suggested by the simulations [35,37].

### C. GWs from the domain wall decay

The peak amplitude and the frequency of GWs are determined by the surface energy density  $\sigma$  (which is a function of the discrete symmetry scale) and the bias term  $\Delta V$  (which explicitly breaks the discrete symmetry and is bound below since domain walls should decay before domination). We use the slope of spectrum  $\Omega_{\text{GW}}^{dw} h^2 \propto f^3$  when  $f < f_{\text{peak}}$  and  $\Omega_{\text{GW}}^{dw} h^2 \propto f^{-1}$  when  $f \geq f_{\text{peak}}$ , as suggested by the estimation of Ref. [10]. The peak amplitude of the GW is [10,38,39]

$$\Omega_{\text{GW}}^{\text{peak}} h^2 \simeq 5.20 \times 10^{-20} \times \tilde{\epsilon}_{\text{gw}} \mathcal{A}^4 \left( \frac{10.75}{g_*} \right)^{1/3} \left( \frac{\sigma}{1 \text{ TeV}^3} \right)^4 \times \left( \frac{1 \text{ MeV}^4}{\Delta V} \right)^2, \quad (4)$$

with the peak frequency [10]  $f^{dw}(t_0)_{\text{peak}} \simeq 3.99 \times 10^{-9} \text{ Hz} \mathcal{A}^{-1/2} \left( \frac{1 \text{ TeV}^3}{\sigma} \right)^{1/2} \left( \frac{\Delta V}{1 \text{ MeV}^4} \right)^{1/2}$ , the area parameter  $\mathcal{A} = 1.2$  [38], the efficiency parameter  $\tilde{\epsilon}_{\text{gw}} = 0.7$  [10], and the effective relativistic degree of freedom at the domain wall decay time  $g_* = 10.75$  [38].

A higher magnitude of GWs is obtained with a large surface energy density. In Fig. 3, the Bayesian fit at  $1\sigma$  sets the bound on the bias term and the surface energy density as follows:  $\log_{10}(\sigma/\text{TeV}^3) \sim [2.79, 4.83]$ ,  $\log_{10}(\Delta V/\text{MeV}^4) \sim [0.26, 4.89]$ . Utilizing  $\sigma \sim 2\sqrt{2}\lambda\eta^3/3$  (here  $\lambda$  and  $\eta$  are the

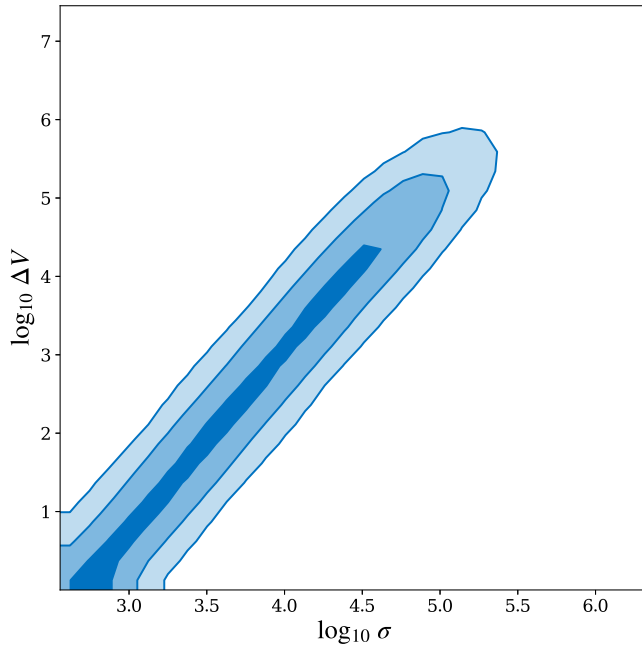


FIG. 3. Constraints on parameters of the domain wall from Bayesian model fitting.

interaction coupling and the breaking scale for the  $Z_2$  discrete symmetry), one can estimate the breaking scale of the discrete symmetry being  $\eta \lesssim 10^2 \text{ TeV}$  for  $\lambda \sim \mathcal{O}(10^{-2})$ .

### D. Scalar-induced GWs

We use the method in Ref. [40] to calculate the energy spectrum of the SGWB resulting from the large scalar fluctuations during inflation and study the constraints from the common-spectrum process detected by NANOGrav. The GW production process happens almost around the horizon reentry of the corresponding modes, after that,  $\Omega_{\text{GW}}$  soon reaches a constant. Assuming a power-law form of scalar fluctuations  $P_{\mathcal{R}}(k) = P_{\mathcal{R}0} k^m$  around  $f = 1 \text{ yr}^{-1}$ , one can simply obtain  $\Omega_{\text{GW}}(t_0, f = 1 \text{ yr}^{-1}) \propto P_{\mathcal{R}0}^2$  and  $\Omega_{\text{GW}}(k) \propto k^{2m}$  from the quadratic  $P_{\mathcal{R}}$ -dependence of  $\Omega_{\text{GW}}(t_0, k)$ .

In the case of scalar-induced GWs, we find  $\log_{10} P_{\mathcal{R}0} \sim [-3.20, -2.10]$  and  $m \sim [-0.89, 0.27]$  are allowed by the NANOGrav data at  $1\sigma$ , as shown in Fig. 4. This shows that the universal behavior in the low-frequency region with  $k^3$  slope [41] is highly disfavored by the NANOGrav data. It is well known that large amplitude scalar perturbations are also responsible for the production of PBHs, which may constitute dark matter and provide merger events of black hole binaries [42–44]. The best-fit  $P_{\mathcal{R}}$  of Gaussian curvature perturbations hints that the abundance of such PBHs is less than  $10^{-12}$  for the PBH mass of about  $0.1 M_{\odot}$ . The constraint on PBH mass function from NANOGrav is much more strict than the others in the same mass range (less than 0.01), such as microlensing results from

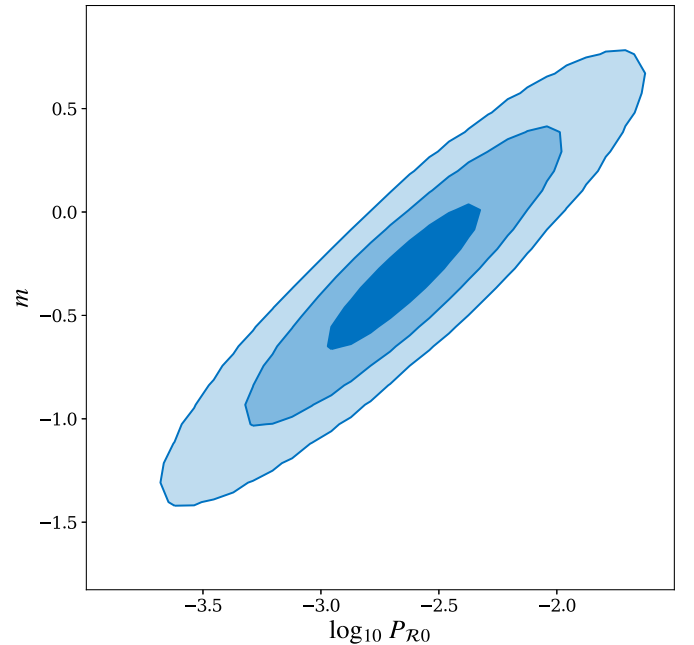


FIG. 4. Constraints on parameters of the power spectrum of curvature perturbations from the Bayesian model fitting.

TABLE I. Bayes factors can be interpreted as follows: given candidate models  $M_i$  and  $M_j$ , a Bayes factor of 20 corresponds to a belief of 95% in the statement “ $M_i$  is true,” this corresponds to strong evidence in favor of  $M_i$  [54].

$B_{ij}$	Evidence in favor of $M_i$ against $M_j$
1–3	Weak
3–20	Positive
20–150	Strong
$\geq 150$	Very strong

EROS/MACHO [45] and OLGE [46]. However, if we consider non-Gaussian scalar perturbations reported in Refs. [47–49], the PBH abundance can be  $10^{-3}$  to explain the merger rate observed by Laser Interferometer Gravitational Wave Observatory (LIGO). The amplitude of scalar induced GWs is also inconsistent with the assumption that PBHs could seed the supermassive black holes [11]. With the amplitude of scalar perturbations extended into smaller scales, the predicted PBH mass decreases and the PBH abundance might increase enormously. PBHs could constitute all dark matter when assuming a scale-invariant power spectrum for scalar fluctuations [50], or explain the microlensing events observed by OGLE when taking into account the early dustlike stage [50].

### III. GW SOURCES COMPARISON

We apply Bayesian model comparison on the following models: SMBHBs, cosmic strings, scalar induced GWs, FOPTs, domain walls, SMBHBs + cosmic strings, cosmic strings + scalar induced GWs, cosmic strings + domain walls, respectively. The result is given in Eq. (5) with the interpretation of Bayes factors given in Table I [51]. We find that the current data shows positive evidence in favor of the cosmic strings explanation against SMBHBs, scalar induced GWs, FOPTs, and domain walls, and weak evidence in favor of cosmic strings against cosmic

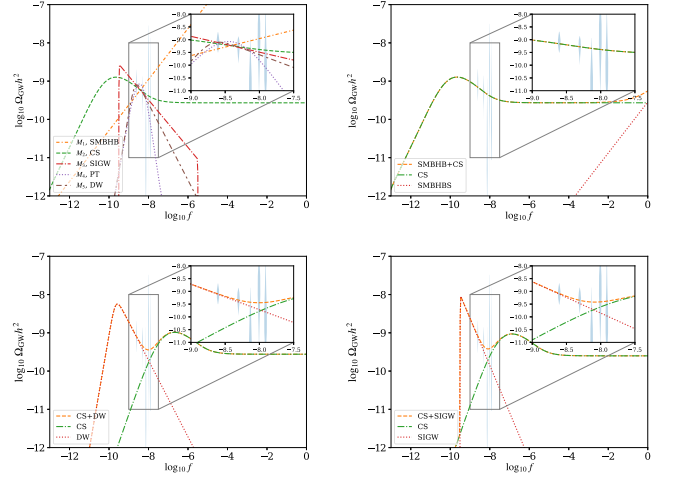


FIG. 5. GW energy spectrum for different models with best-fit value of parameters (which are shown in Supplemental Material [53]). The violin plots show the first five frequency bins of the NANOGrav 12.5-yr data set. The top-left panel shows individual GW source scenario, and the other three plots show the combined explanations with SMBHB + cosmic strings, cosmic strings + domain walls, and cosmic strings + scalar induced GWs.

strings + SMBHBs, cosmic strings + scalar induced GWs, and cosmic strings + domain walls. The data shows a positive evidence of cosmic strings + SMBHBs, cosmic strings + scalar induced GWs, and cosmic strings + domain walls against SMBHBs, see Supplemental Material [53] for details. In comparison with other explanations, there is at least the possibility to explain the common-spectrum process of the GWs from SMBHBs. The GWs spectra of different sources confronted with the low frequency five bins data of the NANOGrav 12.5-yr results are shown in Fig. 5. It shows that the GWs from the cosmic strings fit the data much better due to the fall-off behavior of the GW energy spectrum connecting the matter dominate region (low frequency) and radiation dominate region (high frequency),

$$B_{ij} = \begin{pmatrix} 1 & 0.09 & 0.37 & 0.28 & 0.83 & 0.16 & 0.12 & 0.17 \\ 10.8 & 1 & 3.96 & 3.01 & 8.93 & 1.75 & 1.32 & 1.84 \\ 2.73 & 0.25 & 1 & 0.76 & 2.26 & 0.44 & 0.33 & 0.47 \\ 3.6 & 0.33 & 1.32 & 1 & 2.97 & 0.58 & 0.44 & 0.61 \\ 1.21 & 0.11 & 0.44 & 0.34 & 1 & 0.2 & 0.15 & 0.21 \\ 6.18 & 0.57 & 2.26 & 1.72 & 5.11 & 1 & 0.76 & 1.05 \\ 8.17 & 0.76 & 2.99 & 2.27 & 6.75 & 1.32 & 1 & 1.39 \\ 5.86 & 0.54 & 2.15 & 1.63 & 4.85 & 0.95 & 0.72 & 1 \end{pmatrix}. \quad (5)$$



#### IV. CONCLUSION AND DISCUSSION

In this letter, we evaluate the possibility of the SGWB explanations for the stochastic common-spectrum process observed by the NANOGrav 12.5-yr data set and perform a model comparison based on Bayesian analysis using the five low-frequency bin data. The models include GWs from SMBHBs, cosmic strings, scalar induced GWs, phase transition, and domain walls. We also consider the situation that the SGWB is superposed by two individual sources, including cosmic strings + SMBHBs, cosmic strings + scalar induced GWs, and cosmic strings + domain walls. We evaluate the possibility of these SGWB explanations for the stochastic common-spectrum process observed by the NANOGrav 12.5-yr data set, and the analysis shows that: 1) With positive evidence, the cosmic string model is the most favored one by the current data against SMBHBs and/or other SGWB sources, which hints that the symmetry breaking scale of a  $U(1)$  symmetry of new physics is close to the symmetry breaking scale of the grand unified theory [55–57]; 2) a lot of the parameter spaces for the explanation of the dark sector FOPT is invalidated by the BBN bounds; 3) scalar-induced GWs hint at the mass of PBHs around solar mass and its abundance as dark matter. Other combinations of GWs sources are less supported by data. Noticing that small Bayes factors can be strongly affected by the prior ranges that are assumed for the models, stronger evidence will be obtained with more data available in the future.

References [14,15] study cosmic strings as the possible SGWB sources of the NANOGrav data, and the two studies are performed based on a power-law spectrum. Reference [14] assumes a single  $\alpha_{CS} = 0.1$  and finds  $G\mu \sim [4, 10] \times 10^{-11}$  at  $1\sigma$ . While Ref. [15] assumes  $\alpha_{CS}$  and  $G\mu$  to be free parameters and obtains  $G\mu \sim [6, 17] \times 10^{-11}$  and  $\alpha_{CS} \sim [10^{-2}, 10^{-1}]$  at  $1\sigma$ , our study is based on the Bayesian analysis of NANOGrav data disregarding the power-law spectrum. We show that the NANOGrav 12.5-yr data favors a wider range of  $G\mu$  and a smaller  $\alpha_{CS}$  at  $1\sigma$ , which corresponds to a spontaneous breaking scale of a local  $U(1)$  symmetry closer to the grand unification scale, in comparison with the above two papers, whose GW energy spectrum may be checked in high frequency regions by LIGO, Laser Interferometer Space Antenna, TianQin, and Taiji [58].

#### ACKNOWLEDGMENTS

We are grateful to Xiao Xue, Qiang Yuan, and Xingjiang Zhu for helpful discussions. R.-G. C. was supported by the National Natural Science Foundation of China Grant Nos. 11947302, 11991052, 11690022, 11821505, and 11851302. L. B. was supported by the National Natural Science Foundation of China Grant Nos. 12075041, 11605016, 11947406, and 12047564, the Fundamental Research Funds for the Central Universities under Grant No. 2020CDJQY-Z003, and Chongqing Natural Science Foundation under Grant No. cstc2020jcyj-msxmX0814.

- 
- [1] Z. Arzoumanian *et al.* (NANOGrav Collaboration), *Astrophys. J. Lett.* **905**, L34 (2020).
  - [2] M. Rajagopal and R. W. Romani, *Astrophys. J.* **446**, 543 (1995).
  - [3] E. S. Phinney, [arXiv:astro-ph/0108028](https://arxiv.org/abs/astro-ph/0108028).
  - [4] A. H. Jaffe and D. C. Backer, *Astrophys. J.* **583**, 616 (2003).
  - [5] J. S. B. Wyithe and A. Loeb, *Astrophys. J.* **590**, 691 (2003).
  - [6] X. Siemens, V. Mandic, and J. Creighton, *Phys. Rev. Lett.* **98**, 111101 (2007).
  - [7] A. Kosowsky, M. S. Turner, and R. Watkins, *Phys. Rev. Lett.* **69**, 2026 (1992).
  - [8] C. Caprini, R. Durrer, and X. Siemens, *Phys. Rev. D* **82**, 063511 (2010).
  - [9] L. P. Grishchuk, *Sov. Phys. JETP* **40**, 409 (1975).
  - [10] T. Hiramatsu, M. Kawasaki, and K. Saikawa, *J. Cosmol. Astropart. Phys.* **02** (2014) 031.
  - [11] V. Vaskonen and H. Veermäe, *Phys. Rev. Lett.* **126**, 051303 (2021).
  - [12] V. De Luca, G. Franciolini, and A. Riotto, *Phys. Rev. Lett.* **126**, 041303 (2021).
  - [13] K. Kohri and T. Terada, *Phys. Lett. B* **813**, 136040 (2021).
  - [14] J. Ellis and M. Lewicki, *Phys. Rev. Lett.* **126**, 041304 (2021).
  - [15] S. Blasi, V. Brdar, and K. Schmitz, *Phys. Rev. Lett.* **126**, 041305 (2021).
  - [16] R. Samanta and S. Datta, [arXiv:2009.13452](https://arxiv.org/abs/2009.13452).
  - [17] Y. Nakai, M. Suzuki, F. Takahashi, and M. Yamada, [arXiv:2009.09754](https://arxiv.org/abs/2009.09754).
  - [18] A. Addazi, Y. F. Cai, Q. Gan, A. Marciano, and K. Zeng, [arXiv:2009.10327](https://arxiv.org/abs/2009.10327).
  - [19] W. Ratzinger and P. Schwaller, [arXiv:2009.11875](https://arxiv.org/abs/2009.11875).
  - [20] C. Caprini *et al.*, *J. Cosmol. Astropart. Phys.* **04** (2016) 001.
  - [21] J. Ellis, M. Lewicki, and J. M. No, *J. Cosmol. Astropart. Phys.* **04** (2019) 003.
  - [22] H. K. Guo, K. Sinha, D. Vagie, and G. White, *J. Cosmol. Astropart. Phys.* **01** (2021) 001.
  - [23] J. Ellis, M. Lewicki, and J. M. No, *J. Cosmol. Astropart. Phys.* **07** (2020) 050.
  - [24] C. Caprini, M. Chala, G. C. Dorsch, M. Hindmarsh, S. J. Huber, T. Konstandin, J. Kozaczuk, G. Nardini, J. M. No, K. Rummukainen, P. Schwaller, G. Servant, A. Tranberg, and D. J. Weir, *J. Cosmol. Astropart. Phys.* **03** (2020) 024.
  - [25] J. Ellis, M. Lewicki, J. M. No, and V. Vaskonen, *J. Cosmol. Astropart. Phys.* **06** (2019) 024.
  - [26] M. Hindmarsh, S. J. Huber, K. Rummukainen, and D. J. Weir, *Phys. Rev. D* **96**, 103520 (2017).

- [27] J. R. Espinosa, T. Konstandin, J. M. No, and G. Servant, *J. Cosmol. Astropart. Phys.* **06** (2010) 028.
- [28] M. Hindmarsh, S. J. Huber, K. Rummukainen, and D. J. Weir, *Phys. Rev. Lett.* **112**, 041301 (2014).
- [29] M. Hindmarsh, S. J. Huber, K. Rummukainen, and D. J. Weir, *Phys. Rev. D* **92**, 123009 (2015).
- [30] M. Breitbach, J. Kopp, E. Madge, T. Opferkuch, and P. Schwaller, *J. Cosmol. Astropart. Phys.* **07** (2019) 007.
- [31] Y. Cui, M. Lewicki, D. E. Morrissey, and J. D. Wells, *J. High Energy Phys.* **01** (2019) 081.
- [32] In Ref. [33,34], one can find the case with thermal frictions and particle productions.
- [33] Y. Gouttenoire, G. Servant, and P. Simakachorn, *J. Cosmol. Astropart. Phys.* **07** (2020) 032.
- [34] Y. Gouttenoire, G. Servant, and P. Simakachorn, *J. Cosmol. Astropart. Phys.* **07** (2020) 016.
- [35] J. J. Blanco-Pillado and K. D. Olum, *Phys. Rev. D* **96**, 104046 (2017).
- [36] S. Olmez, V. Mandic, and X. Siemens, *Phys. Rev. D* **81**, 104028 (2010).
- [37] J. J. Blanco-Pillado, K. D. Olum, and B. Shlaer, *Phys. Rev. D* **89**, 023512 (2014).
- [38] K. Kadota, M. Kawasaki, and K. Saikawa, *J. Cosmol. Astropart. Phys.* **10** (2015) 041.
- [39] R. Zhou, J. Yang, and L. Bian, *J. High Energy Phys.* **04** (2020) 071.
- [40] K. Kohri and T. Terada, *Phys. Rev. D* **97**, 123532 (2018).
- [41] R. G. Cai, S. Pi, and M. Sasaki, *Phys. Rev. D* **102**, 083528 (2020).
- [42] B. Carr, K. Kohri, Y. Sendouda, and J. Yokoyama, *arXiv:2002.12778*.
- [43] M. Sasaki, T. Suyama, T. Tanaka, and S. Yokoyama, *Phys. Rev. Lett.* **117**, 061101 (2016); **121**, 059901(E) (2018).
- [44] M. Sasaki, T. Suyama, T. Tanaka, and S. Yokoyama, *Classical Quantum Gravity* **35**, 063001 (2018).
- [45] P. Tisserand *et al.* (EROS-2 Collaboration), *Astron. Astrophys.* **469**, 387 (2007).
- [46] H. Niikura, M. Takada, S. Yokoyama, T. Sumi, and S. Masaki, *Phys. Rev. D* **99**, 083503 (2019).
- [47] R. G. Cai, S. Pi, S. J. Wang, and X. Y. Yang, *J. Cosmol. Astropart. Phys.* **10** (2019) 059.
- [48] R. g. Cai, S. Pi, and M. Sasaki, *Phys. Rev. Lett.* **122**, 201101 (2019).
- [49] N. Bartolo, V. De Luca, G. Franciolini, M. Peloso, D. Racco, and A. Riotto, *Phys. Rev. D* **99**, 103521 (2019).
- [50] G. Domènech and S. Pi, *arXiv:2010.03976*.
- [51] We note that the GW signals from all these SGWB sources that can fit the NANOGrav 12.5-yr results are in tension with the previous bound of PPTA [52] for some parameter spaces, which may be reduced when the improvement of Bayesian priors for the intrinsic pulsar red noise are adopted [1].
- [52] R. M. Shannon, V. Ravi, L. T. Lentati, P. D. Lasky, G. Hobbs, M. Kerr, R. N. Manchester, W. A. Coles, Y. Levin, and M. Bailes *et al.*, *Science* **349**, 1522 (2015).
- [53] See Supplemental Material at <http://link.aps.org/supplemental/10.1103/PhysRevD.103.L081301> for the GWs formula for Scalar-induced GWs, Bayesian model fitting and model comparison.
- [54] R. E. Kass and A. E. Raftery, *J. Am. Stat. Assoc.* **90**, 773 (1995).
- [55] W. Buchmuller, V. Domcke, H. Murayama, and K. Schmitz, *Phys. Lett. B* **809**, 135764 (2020).
- [56] J. A. Dror, T. Hiramatsu, K. Kohri, H. Murayama, and G. White, *Phys. Rev. Lett.* **124**, 041804 (2020).
- [57] S. F. King, S. Pascoli, J. Turner, and Y. L. Zhou, *Phys. Rev. Lett.* **126**, 021802 (2021).
- [58] At last, we comment that the fragmentation of the inflaton could produce GWs during the preheating process [59,60]. At the end of inflation, the inflaton starts to oscillate around the minimum of the effective potential, and the perturbations of the inflaton are exponentially amplified due to parametric resonance. The peak value of  $\Omega_{\text{GW}}$  comes within  $10^{-9}$  to  $10^{-11}$ . However, since the peak frequency of the SGWB is proportional to the inflationary energy scale [61], to generate a SGWB with a peak frequency of  $10^{-9}$  Hz, the inflationary energy scale is below 100 MeV, which is too low to reheat the Universe. Reference [62] shows that the inflationary interpretation of the NANOGrav result is impossible as we comment here.
- [59] S. Y. Khlebnikov and I. I. Tkachev, *Phys. Rev. D* **56**, 653 (1997).
- [60] J. F. Dufaux, A. Bergman, G. N. Felder, L. Kofman, and J. P. Uzan, *Phys. Rev. D* **76**, 123517 (2007).
- [61] R. Easther, J. T. Giblin, Jr., and E. A. Lim, *Phys. Rev. Lett.* **99**, 221301 (2007).
- [62] S. Vagnozzi, *Mon. Not. R. Astron. Soc.* **502**, L11 (2021).